

## STRAINING METAL ELECTRODE AS A SCC TEST. TYPE 304 STAINLESS STEEL IN $MgCl_2$ , $CaCl_2$ AND $LiCl$ SOLUTIONS\*

I. A. MAIER, E. LÓPEZ PÉREZ† and J. R. GALVELE

Departamento de Materiales, Comisión Nacional de Energía Atómica, Avda Libertador 8250-1429-Buenos Aires, Argentina

**Abstract**—Straining metal electrode experiments are a valuable technique for predicting crack propagation rates and crack morphologies when anodic dissolution is the rate-determining step in stress corrosion cracking (SCC). The straining test provides the same information found through more conventional SCC tests, with the advantage of being considerably less time-consuming. In the present work this technique was applied to Type 304 stainless steel in  $MgCl_2$ ,  $CaCl_2$  and  $LiCl$  solutions, tested at room temperature and at 90° and 100°C. The predicted effects of temperature and electrode potential were in good agreement with those reported in the literature. A limit crack propagation rate from about  $10^{-8}$  to  $10^{-7}$   $m s^{-1}$  was found, in agreement with values reported by other authors from fracture mechanic tests. Above the pitting potential the crack propagation rate was found to remain constant, but there was a sharp decrease in the bare metal/filmed metal current ratio, and SCC was replaced by generalized corrosion and pitting.

### INTRODUCTION

IT HAS been pointed out that stress corrosion cracking (SCC), being a kind of heterogeneous electrochemical reaction, should include several steps in its process.<sup>1</sup> One of the possible steps is anodic dissolution, which makes SCC available to evaluation by electrochemical techniques. Under certain conditions the anodic dissolution of the metal at the bottom of the crack becomes the rate controlling step in numerous SCC systems.<sup>2-7</sup> The difficulty of reconciling the idea of anodic dissolution as the controlling process, with the microstructure of the failure surfaces, was pointed out by some authors,<sup>8</sup> but recent publications seem to give an explanation to this point.<sup>9</sup>

A very convenient technique for studying SCC phenomena in a quantitative way is the potentiostatic straining metal technique. This technique is based on the straining wire experiments introduced by Hoar and co-workers<sup>2,3,10,11</sup> and further developed by Galvele and co-workers.<sup>4,5</sup> Hoar and West<sup>10</sup> reported strong electrochemical depolarization when straining stainless steel in  $MgCl_2$  solutions. Scully and Hoar<sup>11</sup> found a qualitative correlation between the current increase of the straining metal and its susceptibility to SCC. Whenever a metal was susceptible to SCC, high current increases were observed upon straining. However, the current densities measured on the wires were of the order of magnitude of 0.1  $mAcm^{-2}$ , too low to account for the empirically found crack propagation rates. By making a few simple assumptions Hoar and Galvele<sup>2</sup> calculated the current density on the fresh metal surface formed during straining. These authors found a good correlation between the propagation rates calculated from the straining experiments and those evaluated

\*Manuscript received 29 September 1981.

†On leave from Michoacana University, Mexico.

from metallographic observations in SCC tests for mild steel in boiling  $\text{Ca}(\text{NO}_3)_2$  and  $\text{NaNO}_3$  solutions. Later Galvele and co-workers<sup>4,5</sup> showed that the ratio of the current density on the bare metal to that on the static metal was a good indication of the corrosion morphology. High current ratios, above 10, were indicative of sharp cracks, while low current ratios, under 5, were associated with generalized corrosion and surface trenching. So far this technique has been successfully applied to the following cases:

(i) mild steel in nitrate solutions<sup>2</sup>; (ii) mild steel in NaOH solutions<sup>3</sup>; (iii) AISI 304 in 1 M HCl solutions at room temperature<sup>4</sup>; (iv) AISI 304 in  $\text{H}_2\text{SO}_4$  plus NaCl solutions at room temperature<sup>5,7</sup>; (v) AISI 304 in boiling 20 N NaOH solution<sup>6</sup>; (vi) Incoloy 800 in boiling 17.5 N NaOH solution<sup>6</sup>; and (vii) Inconel 600 in boiling 17.5 N NaOH solution.<sup>6</sup>

In all these cases the crack propagation rates and crack morphologies predicted by the short term straining experiments were in agreement with those found by conventional SCC experiments.

In the present work, the use of SCC diagrams obtained by the straining electrode technique<sup>4,5</sup> is applied to the study of Type 304 stainless steel in  $\text{MgCl}_2$ ,  $\text{CaCl}_2$  and  $\text{LiCl}$  solutions. SCC of austenitic stainless steels has been reported in these solutions. There is evidence that the anodic dissolution rate on slip steps is the controlling step for SCC in these systems. Potentiostatic SCC tests have shown that there is an applied potential above, but not below which, cracking occurs.<sup>12-15</sup> This potential value lies between  $-0.140$  and  $-0.150$  V (NHE) for  $\text{MgCl}_2$  solutions that boil at temperatures in the range of  $125^\circ$ – $150^\circ\text{C}$ . This critical potential depends on the applied stress and on the presence of other ions in the solution.<sup>15</sup> The existence of a critical potential above which time to failure abruptly decreases has also been found for AISI 304 stainless steel in hot concentrated  $\text{CaCl}_2$  solutions.<sup>16</sup> Electrochemical polarization measurements have shown that Type 304 stainless steel is in the passive condition at potentials close to the corrosion potential in boiling  $\text{MgCl}_2$  and  $\text{LiCl}$  solutions.<sup>17,18</sup> The onset of SCC failures in chloride solutions would then be related to a decrease in the repassivation rate when the passivating film is broken by slip emergence at potentials above the critical or protection potential.

The influence of the solution temperature has also been studied in the present research work, since time-to-failure by SCC is known to be markedly affected by temperature.<sup>16,19,20</sup> Very good correlations were found between the values predicted by the straining electrode experiments, and those reported in the literature.

#### EXPERIMENTAL METHOD

The material used was a 0.08 cm dia. wire of Type 304 stainless steel. The composition of the steel was: Cr 18; Ni 10; Mo 0.25; Fe balance, wt%. The wire was cut into 20 cm long samples some of which were used in the as-received condition. Other probes were annealed at  $1100^\circ\text{C}$  for 15 min under a 200 mmHg argon atmosphere and quenched in water with ice.

Wires with four different surface finishes were employed: (a) wires in the as-received condition, (b) abraded with 600 grade SiC paper, (c) pickled in 15%  $\text{HNO}_3$  + 2% HF solution at  $60^\circ\text{C}$  for 5 min, (d) electropolished for 4 min at 30 V in a refrigerated solution of 90% butil cellosolve + 10% perchloric acid. Immediately before the experiments the wires were cleaned with acetone and dried in hot air.

Except for some small modifications the cell was that described in a previous paper.<sup>21</sup> The solution in the cell was heated by means of an electric resistance coiled around the cell and thermally isolated. The solution was de-aerated in a scrubber connected to the cell. Nitrogen purified according to the

Gilroy and Mayne method<sup>22</sup> was bubbled through the solution and the cell, and after a 2 h de-aeration the solution was introduced into the cell. This de-aeration method was employed in all the tests except those with 40% MgCl<sub>2</sub>, where the solution was de-aerated directly in the cell.

Quasi-potentiostatic anodic polarization curves were drawn by changing the potential in steps of 30 or 40 mV every 5 min. A LYP Electrónica potentiostat and millivoltmeter and a Tacussel recorder were used. In the straining tests, the chosen potential was first applied to the static specimen for periods of 1–30 min and then the wire was strained to breakdown. For potentials close to  $E_p$ , the period at constant potential was always of less than 5 min to prevent crevice corrosion under the stoppers of the cell and pitting of the sample.

The wires were strained in a machine of constant cross head displacement speed, and at initial strain rates of 11, 35, 50, 70 and 92% min<sup>-1</sup>. The cell was coupled to the moving grip of the machine through a pulley, so as to keep the corroding metal inside the cell during straining.<sup>4</sup>

The measurements were made at room temperature, at 90° and at 100°C. The solutions used were: 30% MgCl<sub>2</sub>, 40% MgCl<sub>2</sub>, 35% CaCl<sub>2</sub> and 26.7% LiCl. They were prepared with double distilled water and analytical grade reagents. Potentials were measured through a Luggin capillary with a calomel reference electrode. Potentials are reported on the normal hydrogen electrode scale (NHE). After the tests, the corroded samples were observed with a Philips SEM 500 Scanning Electron Microscope (S.E.M.).

## EXPERIMENTAL RESULTS AND DISCUSSION

### *Quasi-potentiostatic polarization curves*

In this set of experiments the wires used were always in the as-received condition. After the de-aeration period the samples were exposed to the solution for about 1h to get a stable corrosion potential. Then, for room temperature tests, the controlled potential was applied. For high temperature tests, after the de-aeration period, the temperature was increased and kept at the chosen value for at least 10 min before applying the potential.

The behaviour of Type 304 stainless steel was studied in solutions containing a total wt % of 22.34% of chloride ion. The solutions used were 30% MgCl<sub>2</sub>, pH 2.9; 35% CaCl<sub>2</sub>, pH 3.9; and 26.7% LiCl, pH 5.8. Figures 1 and 2 show the polarization curves found at room temperature and at 90°C. A similar electrochemical behaviour was observed in the three solutions, at room temperature. In every case a passive zone was found, followed by a pitting potential. For 30% MgCl<sub>2</sub> solution, the current

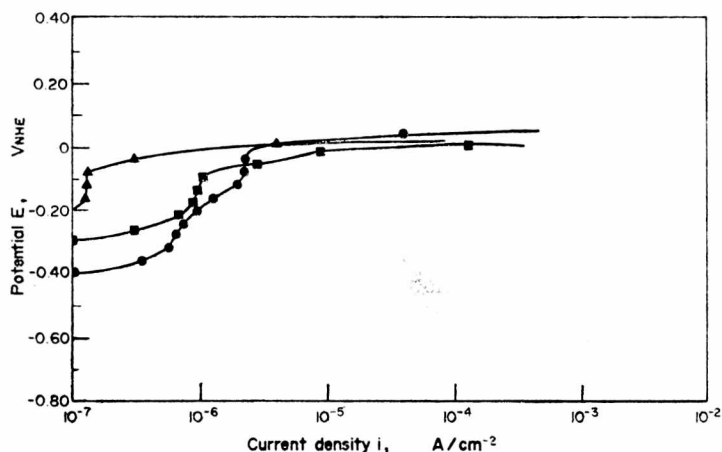


FIG. 1. Measured quasi-potentiostatic anodic polarization curves for Type 304 stainless steel in de-aerated 22.34% chloride solutions at room temperature ( $\blacktriangle$  30% MgCl<sub>2</sub>,  $\blacksquare$  35% CaCl<sub>2</sub>,  $\bullet$  26.7% LiCl).

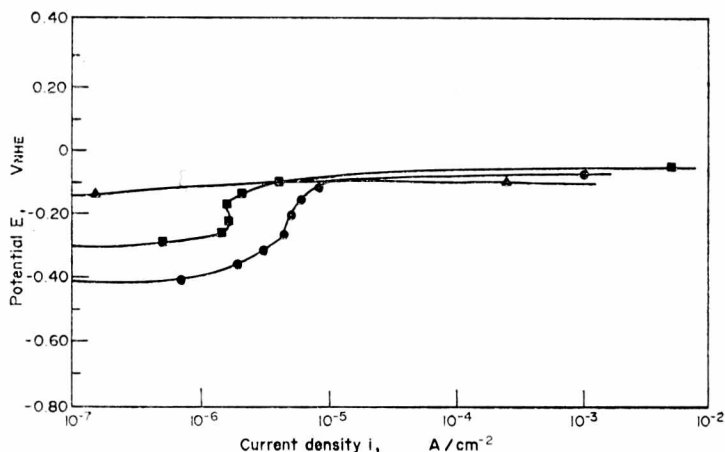


FIG. 2. Measured quasi-potentiostatic anodic polarization curves for Type 304 stainless steel in de-aerated 22.34% chloride solutions at 90°C ( $\blacktriangle$  30%  $\text{MgCl}_2$ ,  $\blacksquare$  35%  $\text{CaCl}_2$ ,  $\bullet$  26.7%  $\text{LiCl}$ ).

density in the passive zone was about one order of magnitude lower than those for  $\text{CaCl}_2$  and for  $\text{LiCl}$  solutions.

At 90°C the corrosion potential of Type 304 stainless steel in the de-aerated 30%  $\text{MgCl}_2$  solution was higher than the pitting potential, and it obscured the passive zone. Similar behaviour was observed in the 40%  $\text{MgCl}_2$  solution at 100°C. The passive current density in the  $\text{CaCl}_2$  and in the  $\text{LiCl}$  solutions increased as a result of the increase in temperature. The effect in the  $\text{MgCl}_2$  solution was obscured by a cathodic reaction.

#### Straining metal experiments

The straining metal electrode technique used to determine the SCC susceptibility was described in former publications.<sup>4-7</sup> If the change in current density during straining is attributed to the reaction on the fresh surface created by the rupture of the oxide film, then we have:

$$(i_s \times A_s) + (i_b \times A_b) = i_y, \quad (1)$$

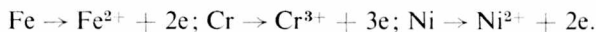
$i_s$  being the current density on the static metal,  $A_s$  the area fraction covered by the film,  $i_b$  the current density on the fresh metal surface,  $A_b$  the fraction of fresh metal surface and  $i_y$  the current density on the straining metal. In the present paper,  $i_b$  was calculated for approx. 20% elongation of the wires.

From the net anodic current density on the metal surface, it is possible to estimate the crack propagation rate by applying the following formula:

$$v_p = i_b \frac{E}{F \cdot d} \quad (2)$$

where  $E$  is the mean electrochemical equivalent weight for AISI 304 stainless steel,

which is  $26.0 \text{ g Eq}^{-1}$  when assuming the following reactions:



$F$  is the Faraday constant and  $d$  is the density of the alloy,  $7.9 \text{ g cm}^{-3}$ .

The values of  $v_p$  and of the ratio  $i_b/i_s$  are the parameters that delineate the potential ranges of susceptibility to SCC.<sup>4-7</sup> When the ratio of the current density on the fresh metal to the current density on the filmed metal is high, a sharp crack can be initiated on those zones of the surface where the film is broken during straining, but when the ratio  $i_b/i_s$  is close to 1, corrosion will take the shape of general attack or pitting. SCC should be expected for values of  $i_b/i_s$  above 10. This means that corrosion will propagate ten times faster at the bottom of the crack than at its sides. On the other hand, if the penetration rate  $v_p$  is small, crack propagation becomes too slow to be detected, and a repassivation process can overtake fresh metal dissolution. This minimum crack propagation rate below which SCC becomes irrelevant depends on the metal-solution system, but seems to be around  $10^{-9}$  or  $10^{-10} \text{ m s}^{-1}$  according to Speidel.<sup>23</sup>

Figures 3 and 4 represent the values of  $v_p$  and the ratio  $i_b/i_s$  as a function of potential for Type 304 stainless steel wires in the as-received surface condition, strained in 22.34%  $\text{Cl}^-$  solutions at 25° and 90°C. In every case the value of the ratio  $i_b/i_s$  is larger than  $10^3$  for potentials below  $E_p$ , thus indicating that sharp cracks could

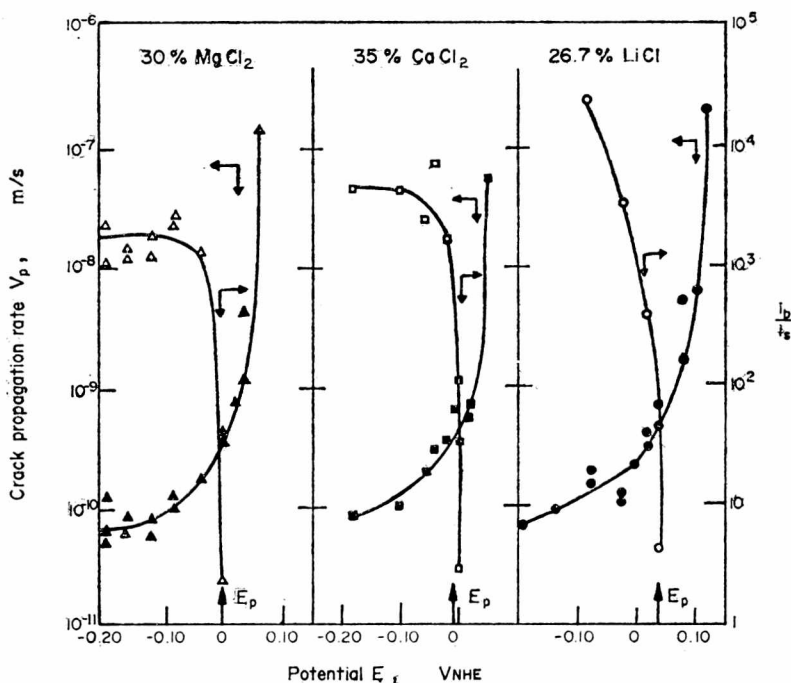


FIG. 3. Calculated crack propagation rates  $v_p$  ( $\blacktriangle$ ,  $\blacksquare$ ,  $\bullet$ ) and fresh metal to filmed metal current density ratios  $i_b/i_s$  ( $\Delta$ ,  $\square$ ,  $\circ$ ) as a function of potential for stressed Type 304 stainless steel in 22.34% chloride solutions at room temperature. Strain rate:  $92\% \text{ min}^{-1}$ .

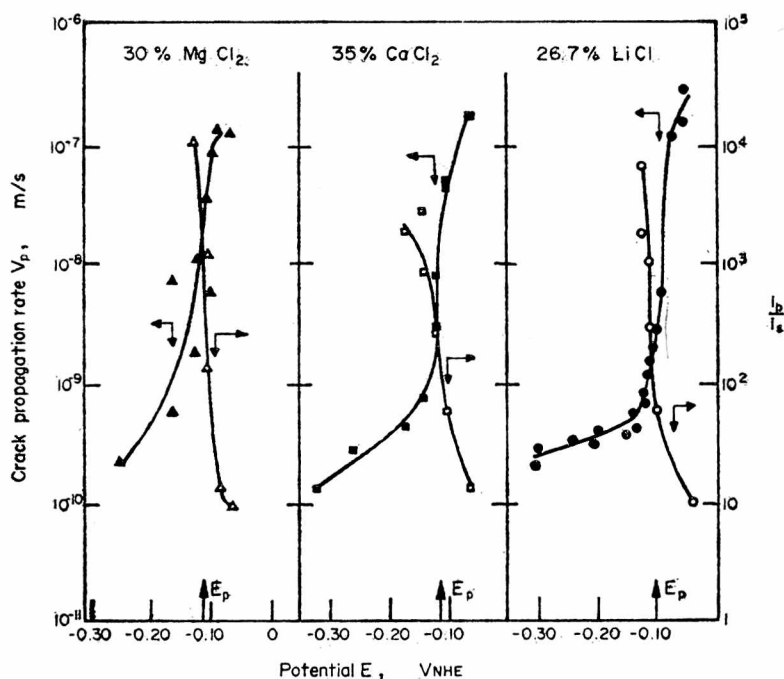


FIG. 4. Calculated crack propagation rates  $v_p$  ( $\blacktriangle$ ,  $\blacksquare$ ,  $\bullet$ ) and fresh metal to filmed metal current density ratios  $i_b/i_s$  ( $\Delta$ ,  $\square$ ,  $\circ$ ) as a function of potential for stressed Type 304 stainless steel in 22.34% chloride solutions at 90°C. Strain rate: 92%  $\text{min}^{-1}$ .

be formed. Above the pitting potential  $i_b/i_s$  decreases rapidly to values below 10 as pitting starts all over the surface.

Figure 3 shows that for the three solutions at room temperature,  $v_p$  at  $10^{-10}$   $\text{m s}^{-1}$  is too low to sustain cracking.

The values at 90°C are one order of magnitude higher than those at room temperature, and they increase as the potential becomes close to the pitting potential. The conditions for SCC are a high  $v_p$  value plus a high  $i_b/i_s$  ratio. At room temperature when one of the values is high, the other is low and vice versa. At 90°C there is a potential range where both values are high, and SCC should be expected. These results agree with the empirical observation that SCC of austenitic stainless steels in chloride solutions is found at high temperatures, while at room temperature it is found only when HCl solutions are being used.<sup>24,25</sup>

The influence of surface roughness and heat treatment on  $v_p$  as a function of potential was studied for Type 304 stainless steel in 30%  $\text{MgCl}_2$  at 90°C and 40%  $\text{MgCl}_2$  at 100°C (Figs. 5a and b). Four different types of samples were tested in the 30%  $\text{MgCl}_2$  solution: (a) wires in the as-received condition (that is, only degreased); (b) samples polished with 600 grade SiC paper; (c) electropolished specimens, and (d) annealed electropolished wires. Figure 5(a) shows that when surface roughness decreases the  $v_p$  vs E curve shifts in the anodic direction; that means that a higher potential is necessary to get the same penetration rate. These results indicate that surface condition has more influence on the steel behaviour than heat-treatment, as

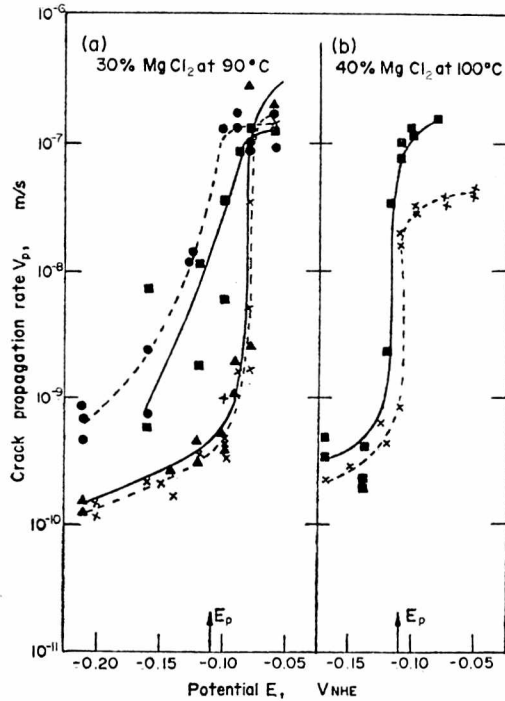


FIG. 5. Calculated crack propagation rates  $v_p$  as a function of potential for Type 304 stainless steel in: (a) 30%  $\text{MgCl}_2$  solution at  $90^\circ\text{C}$ , (b) 40%  $\text{MgCl}_2$  solution at  $100^\circ\text{C}$ . (■ wires in the as-received condition, ● samples abraded with 600 grade SiC paper, ▲ electropolished specimens, × annealed and electropolished wires.) Strain rate:  $92\% \text{ min}^{-1}$ .

the curves obtained for electropolished wires, whether annealed or not, are similar. For all the different types of samples tested we can determine a certain potential value, which depends on the surface condition, above which a limit penetration rate, in the range of  $10^{-7} \text{ m s}^{-1}$ , is attained. This value, estimated from the straining experiments, is in very good correlation with the values of crack penetration rates, in the range of  $10^{-8}$ – $10^{-7} \text{ m s}^{-1}$ , measured by Robinson and Scully<sup>26</sup> and by Speidel.<sup>27</sup>

For the 40%  $\text{MgCl}_2$  solution at  $100^\circ\text{C}$  the behaviour of wires only in the (a) and (d) conditions was compared. A similar shift of the  $v_p$  vs  $E$  curve to more anodic potentials was observed for the electropolished samples. The limit value of  $v_p$  is in the range of  $10^{-8} \text{ m s}^{-1}$ , one order of magnitude lower than in the case of wires without any treatment (Fig. 5b). Some tests were performed on heat-treated and pickled wires. The measured penetration rates are similar to those obtained for non-treated specimens at potentials above the corrosion potential, but  $v_p$  values for the pickled wires are lower at potentials below  $E_c$ .

The above results agree with those reported by other authors: Scheil<sup>28</sup> observed that surfaces prepared by pickling were more resistant to cracking in boiling 42%  $\text{MgCl}_2$  solution than those prepared by mechanical polishing; and Kohl<sup>29</sup> found that for 18–9 Cr–Ni steel in boiling  $\text{MgCl}_2$  solutions, the failure time of electropolished specimens was four times longer than that for specimens having machined surfaces.

Cochran and Staehle<sup>30</sup> obtained somewhat different results: for Type 310 stainless steel exposed in  $\text{MgCl}_2$  solution boiling at  $154^\circ\text{C}$ , wires in the as-received condition were more resistant to SCC than electropolished samples, which in turn, were more resistant to cracking than wires polished with 0 grit polishing paper. They also pointed out that chemically polished specimens with rough surfaces and no cold work exhibited the same hastening of cracking as the mechanically prepared specimens; so they concluded that the decrease in breaking time is due to roughness rather than to the mechanical effect.

There may be different reasons for the influence of surface roughness on the  $v_p$  values as a function of the potential: (a) the actual surface is larger on a rough surface, so that the apparent current density is larger than the real one; (b) the diffusion path for the ionic species that take part in the corrosion process on slip steps, is smaller for smooth specimens. So, according to the local acidification theory<sup>31</sup> the potential should be higher for these samples in order to get the critical proton concentration necessary to initiate the localized attack.

#### *Morphology of the specimens*

Using a scanning electron microscope, the surface morphology of wires strained at  $11\% \text{ min}^{-1}$  in  $35\% \text{ MgCl}_2$ ,  $26.7\% \text{ LiCl}$  and  $30\% \text{ MgCl}_2$  solutions at  $90^\circ\text{C}$  and a  $40\% \text{ MgCl}_2$  solution at  $100^\circ\text{C}$  was compared with samples strained in air. Wires in the as-received condition, annealed and pickled samples and annealed and electropolished specimens were employed.

In the case of wires in the as-received condition slip lines could not be observed due to surface roughness (Fig. 6). Pickled specimens showed a slightly rough surface and some grain boundary attack, and the slip lines were scarcely visible (Fig. 7). On the other hand, slip lines were clearly seen on electropolished wires (Fig. 8).

For samples strained in a  $40\% \text{ MgCl}_2$  solution at  $100^\circ\text{C}$  at potentials close to the pitting potential [between  $-0.080$  and  $-0.100 \text{ V(NHE)}$ ], heavy attack on grain boundaries, twin-boundaries and some slip lines were observed (Fig. 9). Only those slip lines almost perpendicular to the straining direction were attacked. At lower potentials the influence of surface roughness on the penetration rate  $v_p$  was noticed and a larger degree of attack could be seen on a wire in the as-received condition, strained at the  $-0.140 \text{ V(NHE)}$ , than on an annealed and pickled sample, strained at the same potential. After a further decrease in the applied potential no attack was visible. In fact, in that potential range, the calculated penetration rate is in the range of  $10^{-9} \text{ m s}^{-1}$  and the straining time is approx. 160 s, so the attack penetration would be in the order of  $10^{-7} \text{ m}$ .

Another interesting result obtained in the  $40\% \text{ MgCl}_2$  solution is the decrease of  $v_p$  when the solution is prepared several days before the test. This solution is initially saturated at room temperature and it is necessary to heat it above  $80^\circ\text{C}$  to obtain the complete solubility of the salt. However, if the solution is kept at rest for more than two weeks, all the  $\text{MgCl}_2$  dissolves and the pH increases. This effect has poor reproducibility and water absorption from the atmosphere is suspected. An experiment was made with a solution prepared more than a month before the test, and which reached a pH 4.9. An annealed electropolished wire was strained at  $-0.100 \text{ V(NHE)}$  and the  $v_p$  value obtained was two orders of magnitude lower than the value deter-

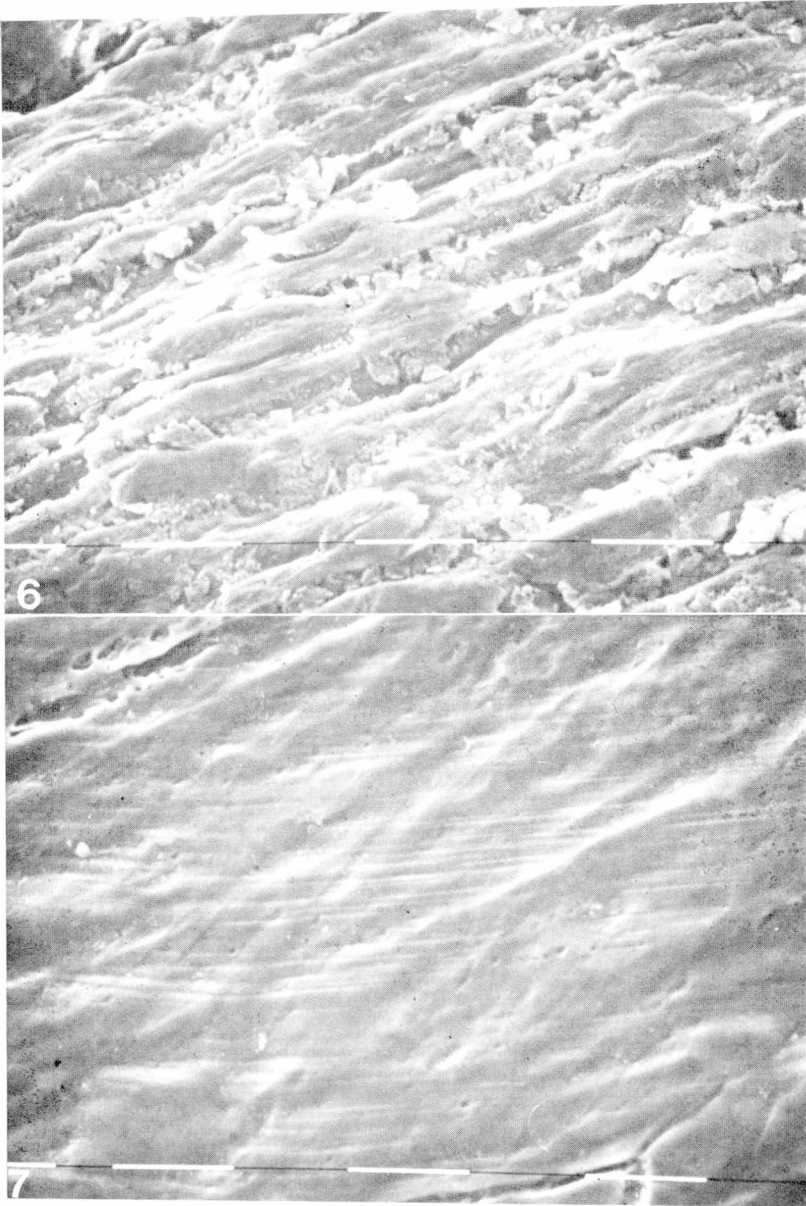


FIG. 6. SEM picture of the surface of a Type 304 stainless steel specimen in the as-received condition, stressed in air. Scale = 10  $\mu\text{m}$ .

FIG. 7. SEM picture of the surface of a Type 304 stainless steel annealed and pickled specimen, stressed in air. Scale = 10  $\mu\text{m}$ .

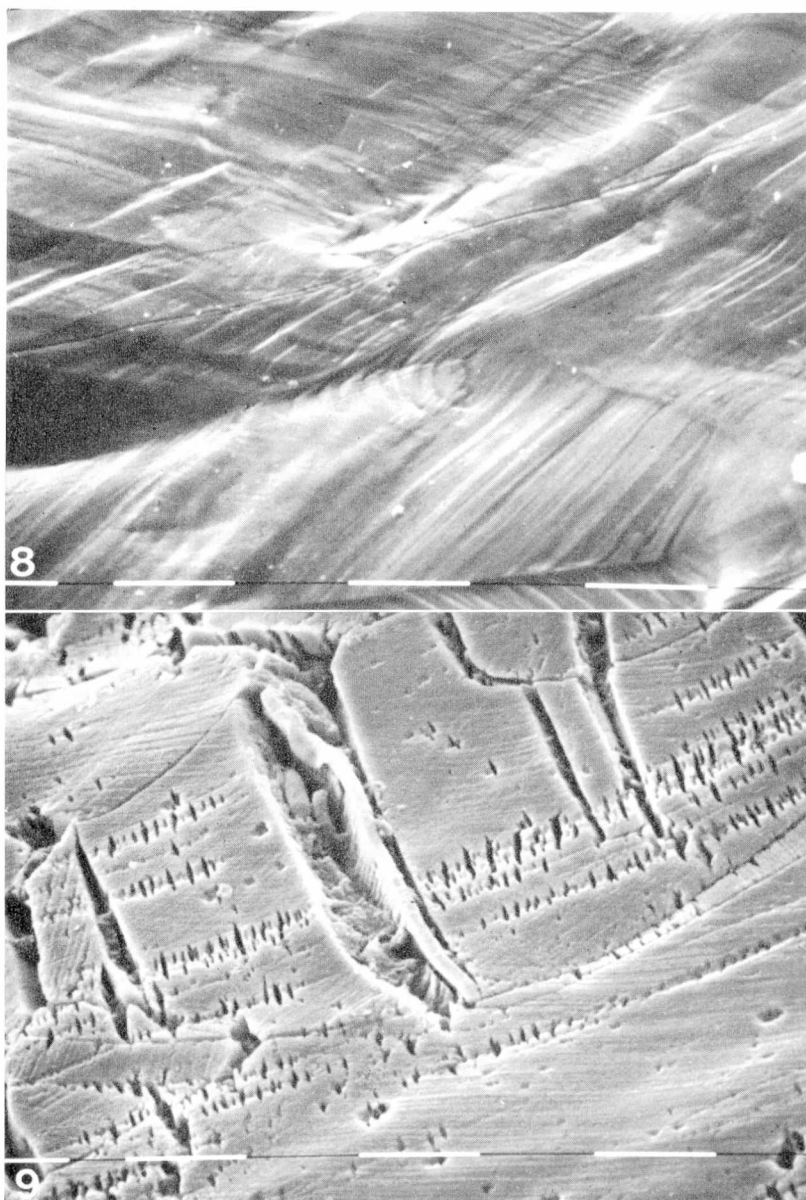


FIG. 8. SEM picture of the surface of a Type 304 stainless steel annealed and electro-polished specimen stressed in air. Scale = 10  $\mu\text{m}$ .

FIG. 9. SEM picture of a Type 304 stainless steel annealed and electro-polished specimen stressed in fresh 40%  $\text{MgCl}_2$  solution at 100°C. Applied potential:  $-0.10 \text{ V(NHE)}$ , strain rate:  $11\% \text{ min}^{-1}$ . Scale = 10  $\mu\text{m}$ .

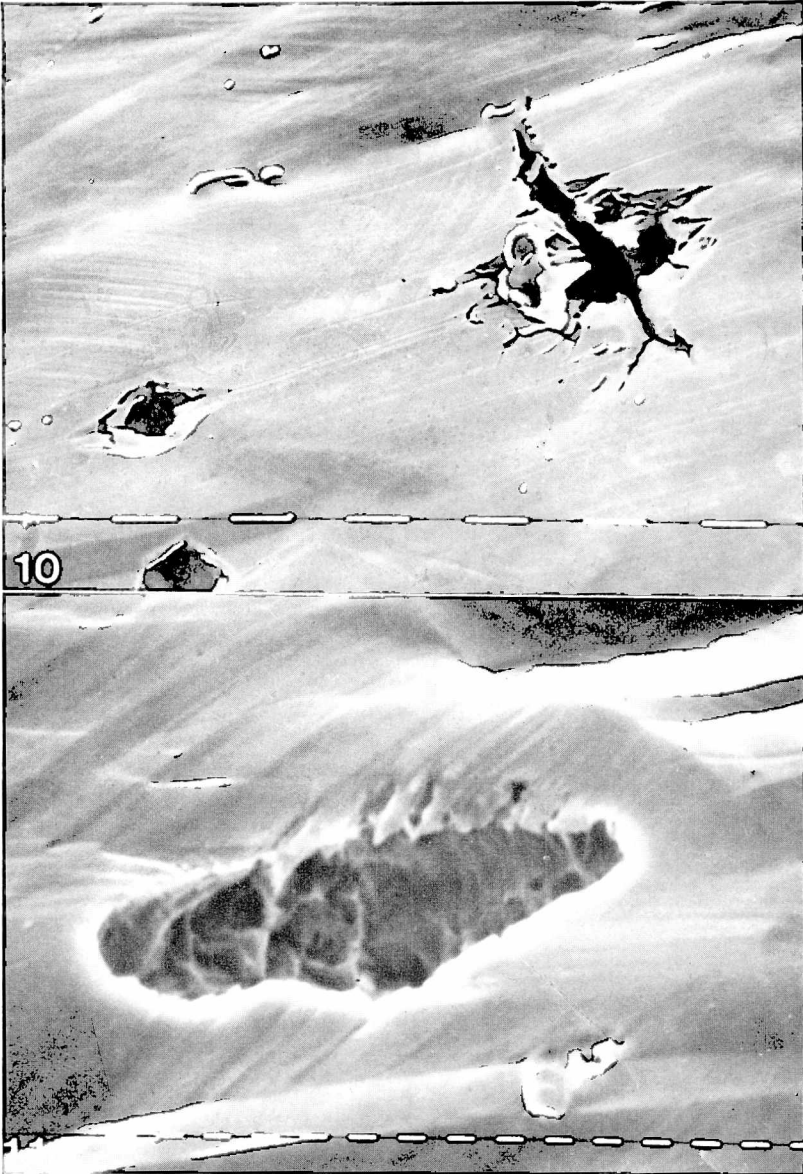


FIG. 10. SEM picture of a Type 304 stainless steel annealed and electropolished specimen, stressed in aged 40%  $\text{MgCl}_2$  solution at  $100^\circ\text{C}$ . Applied potential:  $-0.10$  V(NHE), strain rate:  $11\% \text{ min}^{-1}$ . Scale =  $10 \mu\text{m}$ .

FIG. 11. SEM picture of a Type 304 stainless steel annealed and electropolished specimen stressed in 35%  $\text{CaCl}_2$  solution at  $90^\circ\text{C}$ . Applied potential:  $-0.10$  V(NHE), strain rate:  $11\% \text{ min}^{-1}$ . Scale =  $1 \mu\text{m}$ .



mined in a fresh solution. Scanning electron microscope observation showed that a thick film was formed on the surface, and that it was broken in certain areas where cracks and pits were nucleated (Fig. 10). This type of attack is different from that obtained at the same potential for a fresh solution, as shown in Figs. 9 and 10. These results are similar to those obtained by Silcock and Swann<sup>32</sup> who compared the morphology of samples strained in fresh and preboiled solutions of 42%  $\text{MgCl}_2$  at 150°C. In fresh solutions of low pH values they found attack on slip steps, while in the preboiled solutions the pH increased by evaporation of HCl and the attack was nucleated in non-metallic inclusions.

Type 304 stainless steel strained in the 22.34% chloride solutions at 90°C, showed pitting and some slip line attack, when the potential was held in the 40 mV potential range below the  $E_p$  value determined from polarization curves. Some small cracks nucleated in pits were observed (Fig. 11). For higher potentials severe pitting and general surface attack were obtained.

### CONCLUSIONS

From the results obtained in the present work, we conclude:

- (1) The SCC diagrams drawn by applying the straining electrode technique allow the determination of SCC susceptibility ranges for Type 304 stainless steel in  $\text{MgCl}_2$ ,  $\text{CaCl}_2$  and  $\text{LiCl}$  solutions faster than conventional SCC tests.
- (2) There is good agreement between the crack propagation rates estimated from the straining experiments and those reported by Robinson and Scully<sup>26</sup> and by Speidel.<sup>27</sup> This shows that anodic dissolution is the rate-controlling step in SCC of austenitic stainless steels in the media and in the potential ranges studied in the present work.
- (3) At constant potential, crack penetration rates for Type 304 stainless steel in  $\text{MgCl}_2$  solutions are lower for smoother specimens. The highest penetration rates were measured on specimens mechanically polished with 600 grade emery paper. Attack was lower on wires in the as-received condition and the lowest penetration rates were obtained for electropolished specimens. Similar results were found for electropolished wires, whether annealed or not. This indicates that surface condition is more important in determining steel corrosion behaviour than cold work. This conclusion agrees with the results of Cochran and Staehle.<sup>30</sup>
- (4) An increase in temperature produces an increase in the anodic dissolution rate of the alloy in the chloride solutions. The ratio  $i_b/i_s$  is very high, and by the time it drops to 10, as a result of an increase in the potential, the crack propagation rate is increased by three orders of magnitude. As a result of this, there is a region of potentials where high crack propagation rates coincide with high current ratios, leading to SCC. According to this observation, not only what occurs at the bottom of the crack, but also what occurs with the corrosion rate on the static metal is important in producing SCC.

*Acknowledgements*—This research has been supported by the Comisión de Investigaciones Científicas de la Provincia de Buenos Aires (C.I.C.), by the Servicio Naval de Investigación y Desarrollo, Programa ECOMAR, and by the Proyecto Multinacional de Tecnología de Materiales, OEA-CNEA.



## REFERENCES

1. J. R. GALVELE, Plenary Lecture, 7th Int. Congr. Metall. Corros., Rio de Janeiro, Brazil, October 4-11 (1978).
2. T. P. HOAR and J. R. GALVELE, *Corros. Sci.* **10**, 211 (1970).
3. T. P. HOAR and R. W. JONES, *Corros. Sci.* **13**, 725 (1973).
4. J. R. GALVELE, S. B. DE WEXLER and I. GARDIAZÁBAL, *Corrosion* **31**, 352 (1975).
5. J. R. GALVELE and I. MAIER, *Passivity and Its Breakdown on Iron and Iron Base Alloys* (ed. by R. W. STAEBLE and H. OKADA) p. 178 NACE (1976).
6. J. S. PARK, J. R. GALVELE, A. K. AGRAWAL and R. W. STAEBLE, *Corrosion* **34**, 413 (1978).
7. I. MAIER and J. R. GALVELE, *Corrosion* **36**, 60 (1980).
8. A. J. BURSLE and E. N. PUGH, *Environment-Sensitive Fracture of Engineering Materials* (ed. by Z. A. FOROULIS), The Metallurgical Society of AIME, Warrendale, Pa., p. 18 (1979).
9. T. NAKAYAMA and M. TAKANO, *Corrosion* **37**, 226 (1981).
10. T. P. HOAR and J. M. WEST, *Proc. R. Soc.(A)* **268**, 304 (1962).
11. J. C. SCULLY and T. P. HOAR, 2nd Int. Congr. Metall. Corros., NACE, Houston, p. 184 (1966).
12. H. H. UHLIG and E. W. COOK, JR., *J. Electrochem. Soc.*, **116**, 173 (1969).
13. K. SUGIMOTO, K. TAKAHASHI and J. SAWADA, *Trans. Japan Inst. Metals* **19**, 422 (1978).
14. H. KAESCHE. Private communication.
15. A. GORETSKI and M. SMYALOVSKI, *Prot. Metals* **9**, 223 (1974).
16. S. BRENNERT, *TVF*, **32**, 139 (1961).
17. B. E. WILDE, *J. Electrochem. Soc.* **118**, 1717 (1971).
18. T. P. HOAR and J. E. SLATER, *Corros. Sci.* **14**, 415 (1974).
19. T. P. HOAR and J. G. HINES, *J. Iron Steel Inst.* **182**, 124 (1956).
20. R. L. SHAMAKIAN, A. R. TROIANO and R. F. HEHEMANN, *Corrosion* **36**, 279 (1980).
21. J. R. GALVELE, S. M. DE DE MICHELI, I. L. MULLER, S. B. DE WEXLER and I. L. ALANIS, *Localized Corrosion* (ed. by R. W. STAEBLE), NACE, Houston, p. 580 (1974).
22. D. GILROY and J. E. O. MAYNE, *J. Appl. Chem.* **12**, 382 (1962).
23. M. O. SPEIDEL, *The Theory of Stress Corrosion Cracking in Alloys* (ed. by J. C. SCULLY), NATO, p. 289 (1971).
24. F. MAZZA and N. D. GREENE. Comptes Rendues du 2eme. Symposium Européen sur les Inhibiteurs de Corrosion, Ferrara, Italy, 22-24 Sept., p. 401 (1965).
25. S. TORCHIO, *Corros. Sci.* **20**, 555 (1980).
26. M. J. ROBINSON and J. C. SCULLY, quoted by J. C. SCULLY in ref. 8, p. 77.
27. M. O. SPEIDEL, *Corrosion* **33**, 199 (1977).
28. M. A. SCHEIL, *Corrosion Handbook* (ed. by H. H. UHLIG), John Wiley, New York, p. 179 (1948).
29. H. KOHL, *Corrosion* **23**, 39 (1967).
30. R. W. COCHRAN and R. W. STAEBLE, *Corrosion* **24**, 369 (1968).
31. J. R. GALVELE, *J. Electrochem. Soc.* **123**, 464 (1976).
32. J. M. SILCOCK and P. R. SWANN, ref. 8, p. 133.